RSC Advances

Graphical Abstract

Development of porous and antimicrobial CTS-PEG-HAP-ZnO nano-composites for bone tissue engineering

Arundhati Bhowmick,[a] Nilkamal Pramanik,[a] Piyali Jana Manna,[a] Tapas Mitra,[a] Thirupathi Kumara Raja Selvaraj,[b] Arumugam Gnanamani,[b] Manas Das[c] and Patit Paban Kundu[*a]

Here, we have developed porous, antimicrobial, biodegradable, pH and blood compatible CTS-PEG-HAP-ZnO nanocomposites having good mechanical properties and osteoblast cell proliferation abilities to mimic cancellous bone in bone tissue engineering.

Journal Name
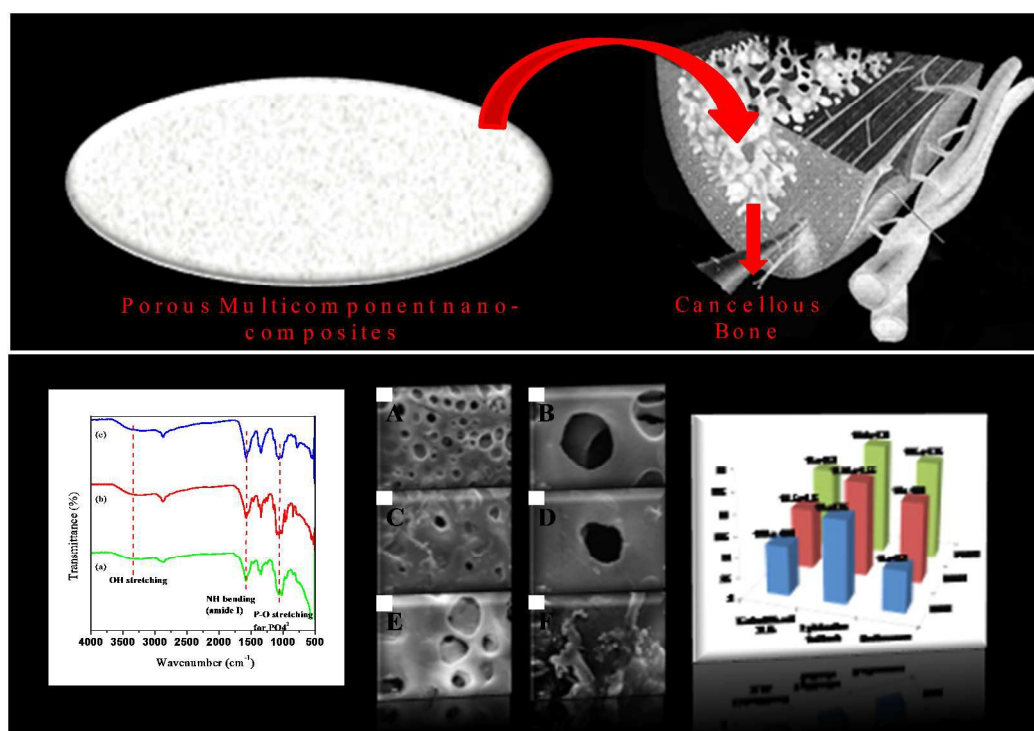
ARTICLE

Development of porous and antimicrobial CTS-PEG-HAP-ZnO nano-composites for bone tissue engineering

Arundhati Bhowmick,[a] Nilkamal Pramanik,[a] Piyali Jana Manna,[a] Tapas Mitra,[a] Thirupathi Kumara Raja Selvaraj,[b] Arumugam Gnanamani,[b] Manas Das[c] and Patit Paban Kundu[*a]

Here, we have developed hybrid nanocomposites of chitosan, poly(ethylene glycol) and nano-hydroxyapatite-zinc oxide with interconnetced macroporous structures for bone tissue engineering. These nanocomposites were characterized by different spectroscopic and analytical techniques. The percentage of porosities and tensile strength of these materials were found to be similar to that of the human cancellous bone. Moreover, these hybrid materials exhibited bio-degradability, neutral pH (7.4) and erythrocyte compatibility. Addition of nano-hydroxyapatite-zinc oxide into the nanocomposites increased antimicrobial activity and protein adsorption ability. The water uptake ability was found to increase with increasing the proportion of poly(ethylene glycol). Finally, osteoblast-like MG-63 cells were grown, attached and proliferated with these nanocomposites without having any negative effect and showed good cytocompatibility.

1. Introduction

Hydroxyapatite [$Ca_{10}(PO_4)_6(OH)_2$, HAP], which has a chemical similarity to the inorganic portion of human bone, has attracted considerable attention in the emerging trend of bone tissue engineering due to its bioactivity, osteoconductivity and biocompatibility.[1] HAP can form a direct chemical bond with neighboring bone tissue and promotes bone formation required for implant osseointegration which is an essential property to reduce damages to surrounding tissues and to increase the implant efficiency.[2] Most biological apatites are non-stoichiometric because of the presence of trace ions such as Mg^{2+}, Mn^{2+}, Zn^{2+}, Na^+, Sr^{2+}, HPO_4^{2-}, CO_3^{2-}. These trace ions have effect on various properties of apatite such as lattice parameters, crystallinity.[3] In this context, one of the primary aims in the field of biomaterials is to get improved quality material for artificial bone substitution which can be achieved by incorporation of additives into HAP. Hence, with the inclusion of trace metal ions such as zinc, silver and manganese into HAP, enhanced its biological performance.[4] Among various metals, synthesis of Zn substituted HAP is of major interest because it is present in abundance as a trace element in bone minerals.[5] Zinc also has properties to support the bone density and impede bone loss.[6] Recent report showed synthesis of zinc oxide doped nano-hydroxyapatite (nano HAP-ZnO) and observe antimicrobial activity against zinc oxide content.[7]

In recent year, extensive research has been done for the fabrication of organic-inorganic materials to mimic natural bone which is composed of the combination of organic collagen fibrils and inorganic nano-hydroxyapatite.[8,9] Among different polymer used, chitosan (CTS, a natural polysaccharide present in chitin in which glucosamine and N-acetylglucosamine units are connected via β (1-4) linkage) is attractive as it is flexible, biocompatible, and nonimmunogenic.[10-12]

However, poor mechanical strength limited its applications in bone tissue engineering. Although, osteogenesis and angiogenic activity was improved by CTS,[13,14] the poorer mechanical strength of CTS[15] makes it impracticable to bear the load similar to the load of bone and it tends to collapse when applied to bone defects in animal model. To improve the mechanical properties, CTS was blended with several synthetic (poly[vinyl alcohol], polycaprolactone, poly [acrylamide], poly[ethylene glycol]) polymers.[16-19] Among these, Poly(ethylene glycol) (PEG) is one of the widely used polymer applied for medical implants. PEG is commonly used in polymer blend as it has several advantages such as its wide range of molecular weights, excellent solubility in water, low toxicity, chain flexibility, and biocompatibility. PEG is readily excreted from the body and forms non-toxic metabolites.[20] Recently nano HAP were embedded in PEG polymeric matrices.[21,22] Though, a few approaches have been made for blending CTS with PEG.[23,24] Therefore fabrication of composites containing CTS and HAP with PEG to obtain a suitable scaffold for bone regeneration is in demand.

Moreover, an ideal scaffold should have interconnected porous structure which can support cell penetration, new tissue ingrowths, nutrient diffusion and neovasculariation, good mechanical property and biocompatibility. Therefore, fabrication of a porous material for successful bone

regeneration is highly desirable.[25-27] In addition, it should have antimicrobial properties for successful bone regeneration to prevent bacterial infection in orthopedic implants. In this context, incorporation of metals having antimicrobial properties such as copper, silver, zinc is becoming frontier area of research. Recent report showed that zinc doped hydroxyaptite can reduce bacterial adhesion.[28] Therefore, in this paper we report development of novel porous multicomponent nano-composites by blending CTS, PEG, nano-HAP-ZnO (CPHZ). The nanocomposites were thoroughly characterized by fourier transform infrared spectroscopy (FT-IR), powder X-ray diffraction (XRD) and scanning electron microscopy (SEM) and investigated their water uptake abilities, porosity, pH, mechanical properties and antimicrobial activities.

2. Results and Discussion

Initially, we have synthesized nano-HAP-ZnO hybrid material by stirring aqueous dispersion of ZnO NPs (20 mg) and HAP (980 mg) at room temperature for 2 hrs followed by drying at 60° for 6 h. The detailed procedure is given in experimental section. The nano-HAP was synthesized by using a wet-chemical precipitation method which was previously reported by us.[29] On the other hand, ZnO NPs were synthesized by condensing $Zn(OAc)_2$ in presence of NaOH following previously reported protocol[30] (See experimental section). The formation of HAP and ZnO NPs were confirmed by FT-IR, powder XRD and SEM studies. Next, we have synthesized different porous nanocomposites (CPHZ I–III) by multicomponent blending of different weight percent of CTS, PEG and HAP-ZnO NPs (Table I) (See experimental section).

**Table 1:** Composition of CPHZ I-III

CPHZs	CTS (wt %)	PEG (wt %)	HAP-ZnO NPs (wt %)
CPHZ I	55	40	5
CPHZ II	55	35	10
CPHZ III	55	30	15

Physicochemical Properties

The physicochemical properties of the synthesized nano-composite materials were investigated by using Fourier transform infrared (FT-IR) spectroscopy, powder X-ray diffraction (XRD) studies. The presence of ZnO NPs was confirmed by characteristic absorption peak at 464 cm^{-1} in the FT-IR spectrum of HAP-ZnO composite (See Fig. 1, ESI-1) whereas bands at 1092 cm^{-1}, 1028 cm^{-1} and 964 cm^{-1} were attributed to phosphate stretching vibration of HAP.

Next, we performed FT-IR of CPHZ I-III. In CPHZ I-III, the absorption band for hydroxyl (O-H) groups present in PEG as well as CTS appeared at in the region of 3300-3350 cm^{-1} as broad band (Fig. 1). In contrast, O-H band for CTS alone was appeared in ~ 3432 cm^{-1}. This lowering of frequency of vibration of the O-H absorption band in composites could be attributed due to intermolecular H-bonding between CTS and PEG. This occurs because the hydrogen bonding pulls on the O-H bond, and dynamically changes the spring constant of that bond. Also bands at 1634, 1637 and 1632 cm^{-1} respectively

were attributed to amide I of CTS (C=O stretching mode along with an N–H deformation mode). Broad bands were appeared for phosphate stretching vibration in HAP at 1132-979 cm^{-1}, 1130-974 cm^{-1} and 1128-970 cm^{-1} respectively. The band corresponding to –O- was appeared at 1078 and that of C-H stretching were at 2873 and 2942 cm^{-1}. These bands indicate the presence of both CTS and PEG in the nanocomposites CPHZ I-III. A detailed comparative study of FT-IR absorption band of individual components and CPHZ I-III was also given in Table 1, ESI-2.
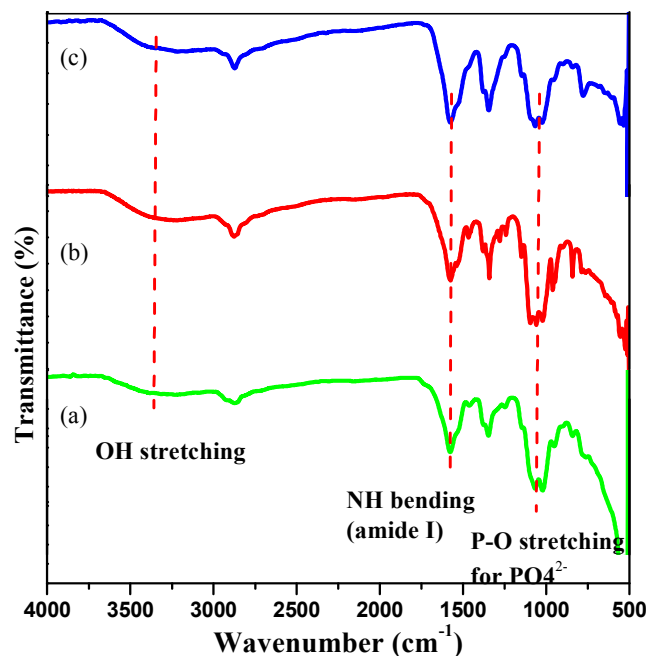

Fig. 1 FT-IR spectra of (a) CPHZ I (b) CPHZ II (c) CPHZ III

The powder XRD study of as-prepared ZnO NPs (Fig. 2a) was studied and presence of peaks at 2θ = 32.18°, 34.02°, 36.67°, 47.95°, 57.01°, 63.26°, 68.33° corresponds to the lattice planes (100), (002), (101), (102), (110), (103), (112) of ZnO respectively. These X-ray diffraction data were in good accordance with reported values.[31] No diffraction peaks of other impurities were detected. In Fig. 2b, characteristic peaks for nano-HAP were observed at 26.51° and 32.57° in powder XRD spectrum of nano-HAP-ZnO.

In vitro degradation test

To eliminate the risk for further surgery, bone tissue engineering composite materials should have the ability to degrade naturally over time as new tissue grows. Therefore, *in vitro* degradation study of CPHZ I was investigated. Along with CTS, another biodegradable polymer, PEG, was added into the nanocomposites. Fig. 3 gives the percentage of weight loss of CPHZ I as a function of soaking time in SBF. The rate of weight loss of CPHZ I from week 1 to week 4 was mainly due to the decrease in the CTS/PEG weight ratio. It was observed that the percentage of weight loss was highest in the first week

i.e. 26 %. After fourth week, 38 % of weight loss of CPHZ I was observed.
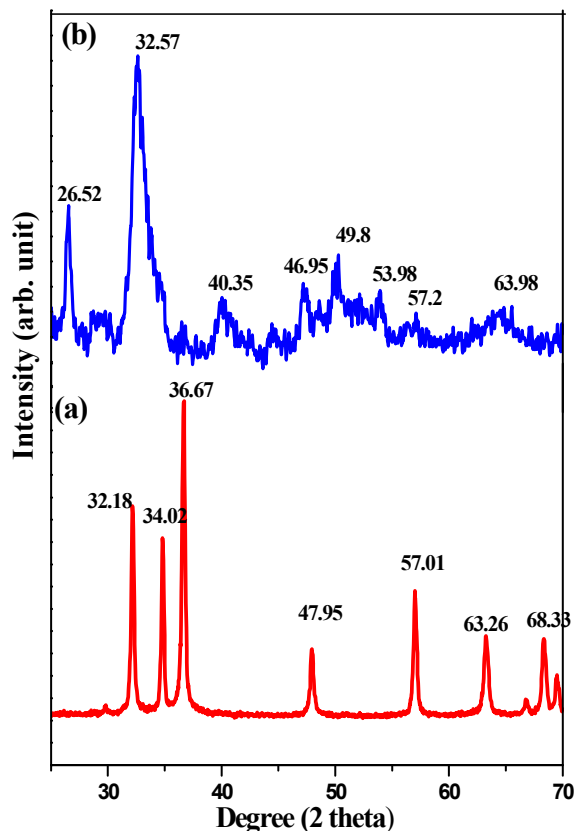
Fig. 2 Powder XRD patterns of (a) ZnO NPs (b) nano-HAP-ZnO
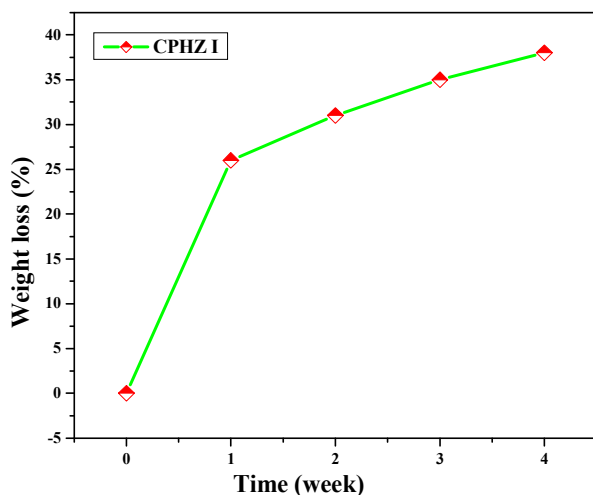
Fig. 3 Percentage of weight loss of CPHZ I as a function of soaking time.

Water uptake (swelling) studies

Water uptake studies of CPHZ I-III were done which is one of the essential properties required for bone tissue engineering applications. The nanocomposites started swelling rapidly within the first hour, signifying good characteristic swelling. Fig. 4 showed that with increasing the amount of PEG (CPHZ III to CPHZ I) from 30 wt % to 40 wt %, the water uptake ability of the composites increased with fixed amount of CTS (55 wt %). Further, it was observed that water uptake abilities of nanocomposites reduced with increasing the amount (5 to 15 wt %) of nano-HAP-ZnO (CPHZ I to CPHZ III). These results are in good agreement with previously reported results.[32] Thus, these composites will serve as good materials for bone tissue engineering.

Microstructure of composites

The size of the ZnO NPs was studied *via* Field emission SEM (Fig. 5). The average sizes of ZnO NPs were in the range of 19-28 nm.
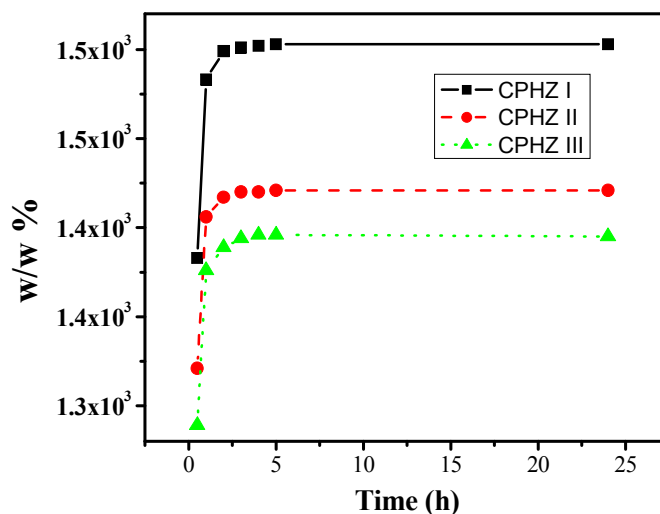
Fig. 4 Water uptake with time of CPHZ I-III

The morphology of CPHZ I-III was also studied through SEM as shown in Fig. 6 where porous structures were observed. The pores were macroscopic in nature, with size of approximately 1 to 10 μm (Fig. 6a, 6c, 6e). It appeared that pores were interconnected with each other (Fig. 6f). On the macroscopic pores walls, many fine pores that have size of less than 1 μm, were also observed (Fig. 6b). This kind of porous structure was observed for silver–chitosan–poly(ethylene glycol) nanocomposites.[33] The presence of ZnO NPs in the nanocomposite was also confirmed by the analysis of Energy-Dispersive X-Ray Spectroscopy (EDS) of CPHZ I. It clearly showed the presence of zinc and oxygen. In addition, it also showed peaks of carbon, calcium and phosphorous (Fig. 2, ESI 3).
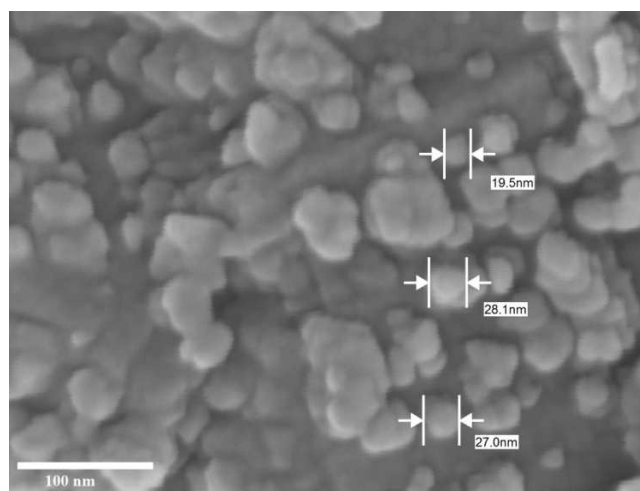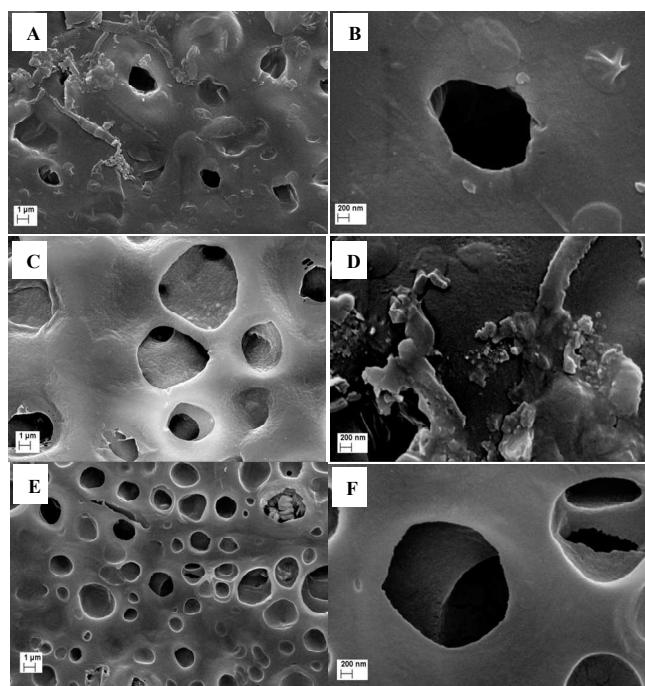
Fig. 5 FESEM image of ZnO NPs

Fig. 6 SEM images of CPHZ I (A & B), CPHZ II (C & D), CPHZ II (E & F).

Porosity and density measurement

Porosity with pore interconnection is necessary for cell infiltration and nutrient exchange.[34,35] Table 2 listed the measured density and porosity of CPHZ I-III. From table 3, porosity of 60.40 %, 67.78 % and 72.25 % for CPHZ I, CPHZ II and CPHZ III respectively was observed. The porosities observed for CPHZ I-III were in the range of cancellous bone (50-90 % porosity).[36] Porosities of CTS membrane was also measured as a control sample and listed in Table 2. It was observed that porosity of CTS (46.10 %) was lower compare to CPHZ I-III.

Table 2 Porosity and density of CPHZ I-III

(CPHZs)	Density (g/cm³)	Porosity (%)
CPHZ I	0.396	60.40
CPHZ II	0.307	67.78
CPHZ III	0.277	72.25
CTS	0.496	46.10

Mechanical properties

The mechanical properties such as tensile strength, percentage total elongation at fracture, Young's modulus and stiffness of CPHZ I-III were determined and listed in Table 3. The tensile strength increased significantly from CPHZ III to CPHZ I, in presence of fixed amount of CTS and with decrease in the amount of nano-HAP-ZnO. With 30 wt % PEG, CPHZ III has tensile strength 10.26 MPa, while with 40 wt % PEG, CPHZ I has 15.83 MPa of tensile strength. The decrease in tensile strength from CPHZ I- CPHZ III is possibly due to the addition of more amount of nano-HAP-ZnO which increased brittleness in the nanocomposites. However, percentage total elongation at break decreased from CPHZ I to CPHZ III (5.50-2.74 %). CPHZ I showed much higher stiffness (87365 N/m) and Young's modulus (1820 MPa) compare to CPHZ II and CPHZ III.

It is well known that porous scaffold is associated with low mechanical strength which restricts its orthopedic application. However, for CPHZ I-III, we observed good mechanical strength along with porosity. Notably, tensile strength, percent elongation at break obtained for CPHZ I-III matches with the tensile strength and percent elongation at break of cancellous bone.[36]

Table 3. Mechanical properties of CPHZ I-III

CPHZs	Tensile Strength (MPa)	Total Elongation at Fracture (%)	Young's Modulus (MPa)	Stiffness (N/m)
CPHZ I	15.83	5.50	1820	87365
CPHZ II	12.54	3.12	708	32132
CPHZ III	10.26	2.74	746	15927

Antimicrobial activities

Next, we investigated the antimicrobial activities of the individual components and CPHZ I-III against gram-negative bacteria *Escherichia coli* XL1B strain and gram-positive strain *Lysinibacillus fusiformis* strain and *Bacillus cereus.* The detailed procedure has been provided in Experimental section.

The antimicrobial activities of CTS, nano-HAP, ZnO NPs, PEG and nano-HAP-ZnO were shown in Fig. 7. All the

individual components except PEG exhibited antimicrobial properties against three different bacterial strain *Escherichia coli*, *Lysinibacillus fusiformis* and *Bacillus cereus*. The maximum bactericidal activity was observed for ZnO NPs against *Bacillus cereus*.

Fig. 8 represented the antimicrobial activities of CPHZ I-III where antimicrobial activities increased with increasing the nano-HAP-ZnO content that is CPHZ I to CPHZ III. With CPHZ III (15 wt % nano-HAP-ZnO), zone inhibition for cell growth was 12.0±0.57, 11.4±0.77 and 11.6±0.75 against *Escherichia coli*, *Lysinibacillus fusiformis* and *Bacillus cereus* respectively.
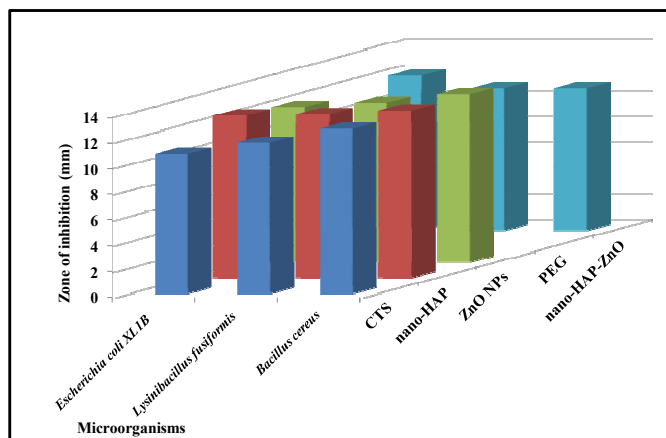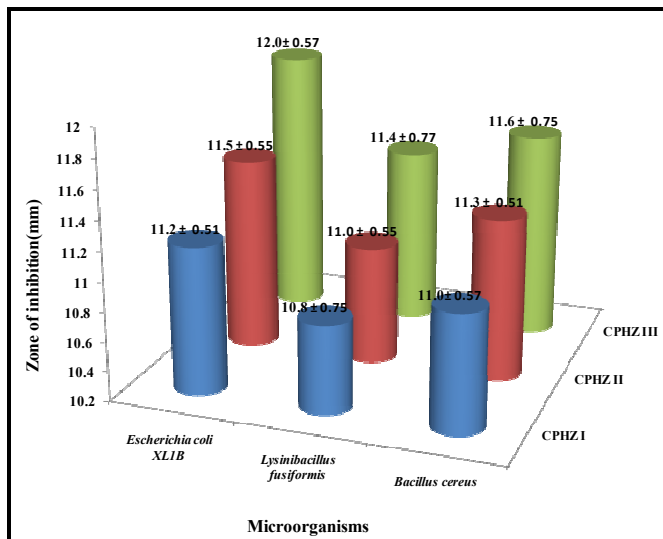

**Fig. 7** Antimicrobial activities of CTS, nano-HAP, ZnO NPs, PEG and nano-HAP-ZnO

These results suggest that the cell-growth inhibited effect was more prominent in case of gram-negative bacteria strains (*Escherichia coli*) compare to gram-positive strains. The better inhibitory effect on gram-negative strain compare to gram-positive strain was due to the presence of a thicker peptidoglycan cell-wall in gram positive bacteria, which protects inner parts of the cell from the penetration of CPHZ I in the cytoplasm.[37] Overall, CPHZ I-III exhibited good antimicrobial properties which are essential to prevent bacterial infection in orthopedic implants for successful bone regeneration.

pH study

6.2 mg of CPHZ I was taken in a bottle filled with 30 ml (150 mM) physiological saline solution, which was setting for stirring continuously at 37 °C. The pH of the solution was measured by a pH meter periodically upto 14 days. The changes of the pH values from 1 to 14 days were given Fig. 9. It can be concluded from the above study that the pH value of CPHZ I was equal to the human plasma (pH 7.4), therefore the nanocomposite should be nontoxic to an organism in the human body. There is not much change in pH value (ranging from pH 6.8-7.42) observed from the day 1 to day 14. Thus, a low alkalinity pH (7.4) of CPHZ I, similar to the pH of human plasma, is very much desirable for the application in bone tissue engineering.

Fig. 8 Antimicrobial activities of CPHZ I-III
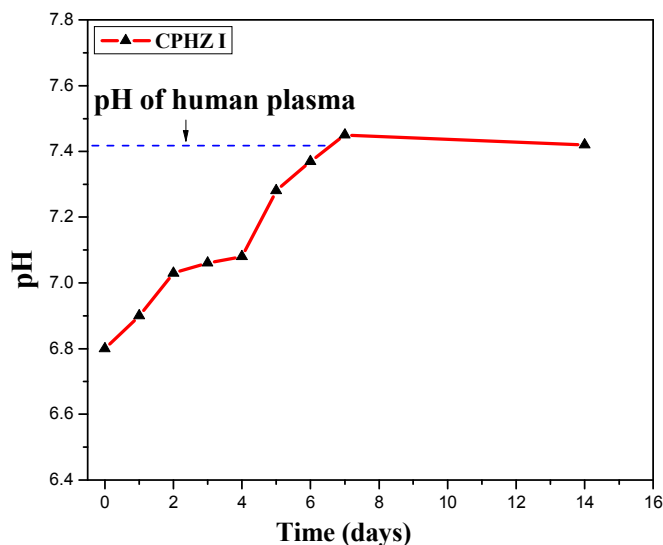
Fig. 9 pH study of CPHZ I

Hemolytic assay

The hemolysis assay is a significant test for the materials used in biomedical application which might be exposed in blood environment and damaged the erythrocytes in certain degree. For the present study the assay was carried out to evaluate the blood compatibility of CPHZ I. The detailed procedure was given in experimental section. The results in Fig. 10 showed that there was no damage of erythrocytes in presence of CPHZ I which confirmed that prepared biopolymer is compatible with erythrocytes.
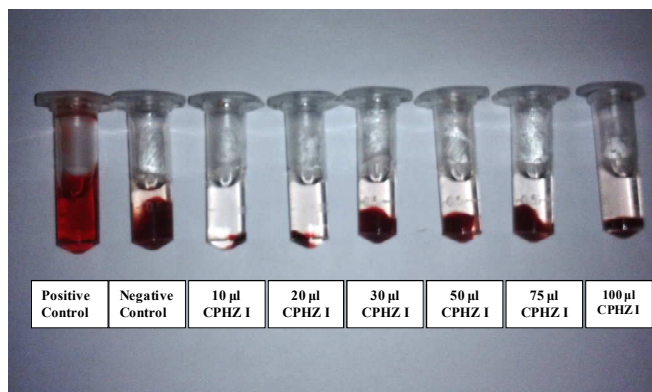
Fig. 10 Hemolysis studies of CPHZ I. Positive control (50 µl RBC + 950 µl H₂O, negative control (50 µl RBC + 950 µl PBS) and 10, 20, 30, 50, 75 and 100 µl of CPHZ I was made upto 950 µl with PBS and then 50 µl of RBC sample was added and mixed.

Protein adsorption study

The BSA adsorption results showed that the maximum protein adsorption was found to be 66.34 % for CPHZ III having 15 wt % of nano-HAP-ZnO content after 24 hours (Fig. 11). This could be due to the fact that the addition of nano-HAP-ZnO would have increased the surface area of the nanocomposites, and hence more proteins were adsorbed. The BSA adsorption onto CPHZ II and CPHZ III was found to be 62.13 % and 66.34 % respectively (Fig. 11). The result was in good accordance

with the result of porosity measurements where percentage of porosity increased from CPHZ I to CPHZ III, therefore increased the surface area of the nanocomposites and improved the protein adsorption. Increased protein adsorption of the nanocomposites would lead to have better cell matrix interaction, adhesion and spreading on the scaffolds.[38]
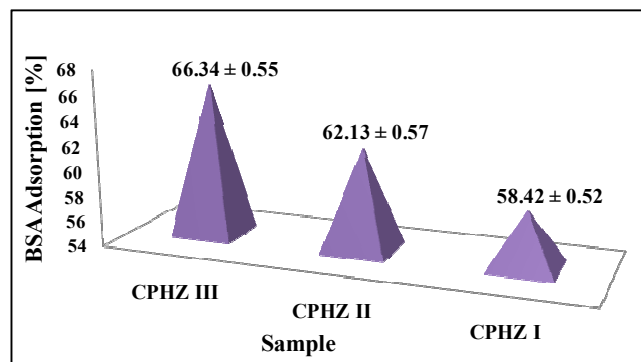
Fig. 11 Protein adsorption study of CPHZ I-III.

***In vitro* cell proliferation study and MTT assay**

With reference to the cytotoxicity of the prepared nanocomposites CPHZ I and CPHZ III, cell proliferation assays were carried out. MTT assay was done to check the toxicity of the prepared nanocomposites (CPHZ I and CPHZ III).
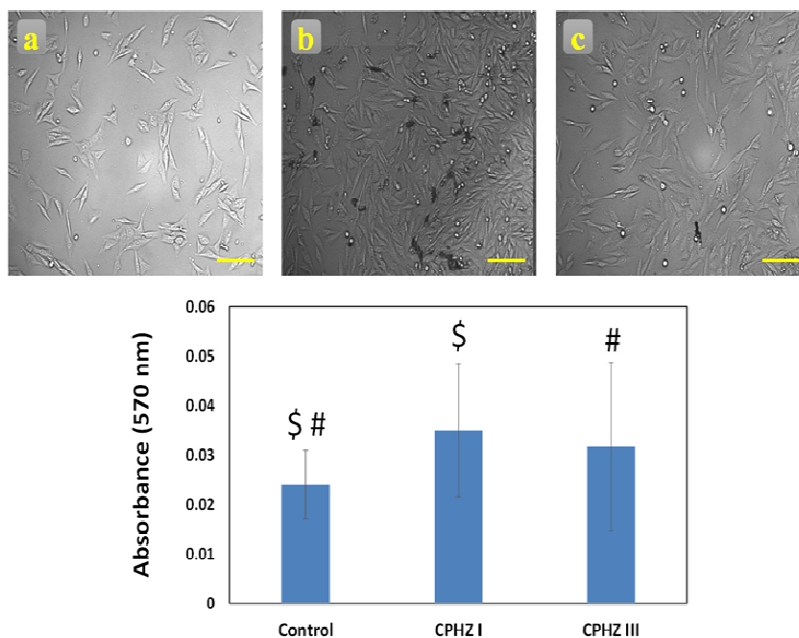
Fig. 12 Inverted phase contrast micrographs of MG-63 cells grown over (a) non coated (control), (b) CPHZ I and (c) CPHZ III coated tissue culture plate for 24 h. The scale bar measures 0.1 mm. (all the values are the mean ± SD of triplicates) and MTT assays for proliferation of MG63 cells cultured with scaffolds after 24 h, compared with the control (without scaffolds) under the same culture condition. ($, #) $p < 0.05$, compared to control.

The cell viability of CPHZ I and CPHZ III were higher than that of control. This might be due to addition of hydroxyapatite crystals in the scaffold. The cell proliferation of MG-63 on CPHZ I and CPHZ III scaffolds was observed to be high as compared control (Fig. 11). This indicates that the newly developed scaffolds benefit for the osteoblast-like cells growth, attachment and proliferation, and there was no significant difference among the uncoated and coated scaffolds. The biocompatibility assessment demonstrated that the modified scaffolds had no negative effect on osteoblast-like MG-63 cells and showed good cytocompatibility.

3. Experimental section

Materials

Chitosan was purchased from Acros Organics. Molecular weight of CTS was 230 kDa, determined by the well-known Ubbelohde viscometric methods. Degree of deacetylation (DDA) of CTS was 86% and it was determined by potentiometric titration method. Nano-hydroxyapatite (nano-HAP) was synthesized following the protocol reported in our previous paper.[29] For the synthesis of nano-HAP, calcium nitrate tetrahydrate [$Ca(NO_3)_2.4H_2O$], diammonium phosphate [$(NH_4)_2HPO_4$], and 25% ammonium hydroxide were purchased from Merck. For the synthesis of zinc-oxide nanoparticles, zinc acetate [$Zn(OAc)_2$], sodium hydroxide [$NaOH$] were purchased from HiMedia Private Ltd. Polyethylene glycol (PEG) was purchased from Merck, has molecular weight 20000.

Detailed experimental procedure for the synthesis of chitosan-PEG-nano-HAP-ZnO porous multicomponent nano-composites (CPHZs)

Synthesis of ZnO nanoparticles (NPs)

Synthesis of ZnO NPs was done following a reported procedure.[30] 0.45 M aqueous solution of zinc acetate $Zn(OAc)_2$ and 0.9 M aqueous solution of NaOH were prepared in distilled water. Then the beaker containing NaOH solution was heated to about 55^0C. Then zinc acetate solution were added drop-wise (slowly for 1 hr) to the above heated solution under high speed stirring. The beaker was sealed at this condition for additional 2 hrs and the precipitated ZnO nanoparticles were cleaned with deionised water and ethanol & then dried in air at $60\ ^0C$.

Synthesis of nano-HAP-ZnO

Aqueous solutions of 20 mg of ZnO NPs and 980 mg of nano-HAP were prepared and mixed. The mixed solutions were stirred vigorously for two hours. The obtained suspensions were filtered and dried in a hot air oven at $60\ ^0C$ for 6 h.

Synthesis of chitosan-PEG-nano-HAP-ZnO porous multicomponent nano-composites (CPHZs)

For the synthesis of CPHZ I-CPHZ III, a fixed amount of CTS (55 wt %) were dissolved in 15 ml of 85 % formic acid with stirring for 2 hours. After that different amount of PEG (40, 35, and 30 wt %, respectively) and HAP-ZnO NPs (5, 10, and 15 wt %, respectively) were added to the CTS solution. The resulting mixture was stirred vigorously overnight to get a homogenous mixture of the composites. It was then transferred to petri-dishes for formic acid evaporation at room temperature to get the film. It was then dried at $60\ ^o C$ for 48 h.

Characterizations

Fourier Transform Infrared Spectroscopy (FT-IR) study was carried out with Attenuated Total Reflectance (ATR)–FT-IR spectrophotometer (model alpha, Bruker, Germany). All spectrums were recorded with scanning range from 4000 to 500 cm^{-1}. X-ray diffraction patterns of CPHZ I-III were obtained by using X-ray diffractometer (Goniometer Miniflex, JAPAN). The samples were tested at 30 Kv and 15 mA with Cu Kα radiation. The relative intensity was recorded at a 2θ of 4°/min and in the range of 5° to 70°.

The in vitro degradation study of CPHZ I was conducted in a simulated body fluid (SBF) medium composed of (per lit) NaCl (7.996 g), NaHCO$_3$ (0.350 g), KCl (0.224 g), K$_2$HPO$_4$.3H$_2$O (0.228 g), MgCl$_2$. 6H$_2$O (0.305 g), CaCl$_2$ (0.278 g) and Na$_2$SO$_4$ (0.071 g). 1000 ml of saline solution was buffered at physiological pH 7.4 at 37^oC with tri-(hydroxyl-methyl) amino-methane (6.057 g) and hydrochloric acid. The ionic strength of the as prepared fluid solution was very close to those of human blood plasma. For the degradation study, the dried samples were weighed and immersed in a vial containing 10 ml of SBF solution and it was kept at 37.0 ± 0.5^oC water baths under constant shaking. Then, the soaking capability of the respective samples was monitored for 1, 2, 3 and 4 weeks and withdrawn from SBF. Finally, it was gently rinsed with de-ionized water and weighed again after being dried. The rate of weight loss (W$_L$) was calculated according to the formula-

$$W_L = [(W_0-W_1)/\ W_0] \times 100\%,$$

Where, W$_0$ and W$_1$ denote the weight of the sample before and after soaking, respectively.

For the study of water uptake abilities of CPHZ I-III, five replicates were used for each study. At first, dry scaffolds were weighed (W_d) and immersed in distilled water. Then, the scaffolds were gently blotted with filter paper to remove the excess water and weighed (W_w) again after 0.5, 1, 2 3, 4, 5 and 24 hours to determine water uptake. The percentage of water absorption (E$_A$) of the composites at equilibrium was calculated using Equation (1)[39]:

$$E_A = [(W_w - W_d)/\ W_d] \times 100 \qquad \dots\dots\dots (1)$$

The size of ZnO NPs (Fig. 4) was examined using a field emission scanning electron microscope (FESEM) (JEOL JSM7600F). For FESEM examination, sample was sputtercoated with gold using E-1010 Hitachi Ion Sputter (Made in Japan). The structural morphology of CPHZ I-III was examined using a scanning electron microscope (SEM) (Model EVO-18, Carl-Zeiss, Germany). For SEM examination, dry samples were coated with gold layer using a Hitachi sputter 80 coater (model-E1010 Ion sputter, made in Japan).

Porosity and density of the prepared scaffolds were determined by the liquid displacement method.[40] Initially, the volume of the ethanol (V$_1$) and dry weight (W) of the scaffolds were measured. The scaffolds were then immersed into the dehydrated alcohol for 25 h until it was saturated by absorbing the alcohol, and the scaffolds were weighed again. The total volume of the ethanol and scaffold was then recorded as V$_2$. Then, the scaffold was removed from the ethanol and the residual ethanol volume was measured as V$_3$. In addition, to measure the volume of ethanol adsorbed by the bulk materials of the CPHZ I-III, we have weighed the dried scaffolds after removing from ethanol. The measured volume of ethanol was added to V$_3$.

The density (d) of the scaffold was expressed as:

$$d = W/\ (V_2- V_3) \qquad \dots\dots\dots\dots (2)$$

The porosity (ε) of the samples was calculated based on the following formula:

$$\varepsilon = (V_1 - V_3)/(V_2 - V_3) \qquad \ldots\ldots\ldots\ldots (3)$$

Mechanical properties of CPHZ I-III were measured using a Universal Testing Machine (UTM) of Lloyd Instruments Ltd. (Model LR01KOLPLUS, ENGLAND). These tests were performed in tensile mode. The measurements were performed with a cross-head speed of 5 mm/min with 30-mm gauge length at room temperature. Width and thickness of each sample were measured before testing. At least five specimens were tested for each sample. The dimensions of scaffolds were 18 mm in diameter and 0.08 mm in thickness. Tensile strength, Young's modulus, stiffness and percentage elongation at break were obtained from tensile testing.

For the antimicrobial study, the test bacterial cultures, *Escherichia coli* XL1B strain (gram-negative), *Lysinibacillus fusiformis* strain (gram-positive) and *Bacillus cereus* (gram-positive strain) were collected from the Department of Microbiology, University of Calcutta. CPHZs were tested for antimicrobial activity by disk diffusion method[41] against *Escherichia coli* XL1B strain (gram-negative), *Lysinibacillus fusiformis* strain (gram-positive) and *Bacillus cereus (*gram-positive). The inhibitory effect was tested on a sterilized agar plate of liquid nutrient broth medium which contains animal tissue (5.0g/l), NaCl (5g/l), beef extract (1.5g/l) and yeast extract (1.5 g/l). The broth was solidified by using 1.3g/l of agar. Approximately 10^5 colony-forming units (CFU) of each strain (gram positive and gram negative bacterial strain) was swabbed uniformly on an agar plate using sterile cotton swabs to incubate at $37^{\circ}C$. Different sets of composite films were cut into spherical shaped and placed it after sterilization onto each of selected zones of the agar plate and kept for 24 hours to observe the bactericidal effect on those microorganisms at $37^{\circ}C$.

Blood compatibility of CPHZ I was examined by hemolysis assay. Fresh human blood was used for this study. It was centrifuged at 3000 rpm for 10 min at $4^{\circ}C$. The RBC pallet was then washed with PBS solution to adjust the pH at 7.4 and centrifuge in the same way. One type of substance will cause lysis of the RBCs leading to the release of hemoglobin in presence sample. The cell debris and intact cells were separated by centrifugation. The amount of hemoglobin corresponds to the number of cells lysed by CPHZ I. At first different amounts of samples in tubes (10, 20, 30, 50, 75, 100 μl) were taken and made up to 950 μl with PBS. After that, 50 μl of RBC sample was added and mix. The samples were incubated in dark for 10 minutes and then centrifuged for 10 minutes at 6,000 rpm. The OD values of the supernatant were measured at 540 nm using a spectrophotometer. The obtained sample values were compared with Positive control (50 μl RBC + 950 μl H_2O) and negative control (50 μl RBC + 950 μl PBS). Each concentration was evaluated in triplicate.

The surface adsorptions of protein on the surface of nanocomposites [CPHZ I, CPHZ II and CPHZ III] were investigated by incubating the films separately in 5 ml (2mg/ml) of bovine serum albumin (BSA) solution for 24 hours at $37^{\circ}C$. About 300 μl of protein solution was withdrawn from the sample solution within a definite time interval and the change of concentration of solution was recorded by using a UV-Visible spectrophotometer at 280 nm.

For in vitro cell proliferation study and MTT assay, MG-63 cells, procured from NCCS, Pune, India, were used. MTT (3-(4,5-dimethylthiazol-2-yl)-2,5-diphenyltetrazoliumbromide) was procured from Sigma Aldrich. The cultures were maintained in DMEM supplemented with 10% Fetal Bovine Serum (FBS), 200 mM Glutamine, 2 mg ml^{-1} sodium bicarbonate and $1\times$ antibiotic and antimycotic solution. Periodically the medium was replaced. The cells were cultured in tissue culture flasks and incubated at 37°C in a humidified atmosphere of 5% CO_2. Trypsin at 0.05% was used to detach the cells. For cell proliferation study (MTT assay), cells were grown in DMEM (Dulbecco's modified Eagle's medium) supplemented with 10% (v/v) fetal bovine serum and 1% antibiotic and were incubated at 37°C in 5% CO_2 humidified atmosphere. Polystyrene 96 well culture plates (Tarson, India) were coated with CPHZ I and CPHZ III solutions. The plates were dried in a laminar airflow hood followed by the UV sterilization. The cells were seeded at the density of 0.5×10^6 per well and incubated at 37°C in a humidified atmosphere containing 5% CO_2. After 24 h of incubation, the supernatant of each well was replaced with MTT diluted in serum-free medium and the plates were incubated at 37°C for 4 h. After removing the MTT solution, a mixture of acid and isopropanol (0.04 N HCl in isopropanol) was added to each well and pipette up and down to dissolve all of the dark blue crystals and then left at room temperature for few minutes to ensure all crystals were dissolved. Finally, absorbance was measured at 570 nm using a UV spectrophotometer. Each experiment was performed at least three times. The sets of three wells for the MTT assay were used for each experimental variable.

Conclusions

In conclusion, porous multicomponent nanocomposites (CPHZ I-III) were fabricated containing CTS, PEG, nano-HAP-ZnO. FT-IR studies and X-ray diffraction study confirms the presence of individual components. SEM revealed interconnected macro porous structure. The water uptake ability of the CPHZ I-III was found to increase with increasing the amount of PEG. pH study indicated that CPHZs are nontoxic to the human body having pH similar to the human plasma. The tensile strength increased significant from CPHZ III (10.26 MPa) to CPHZ I (15.83 MPa). Total elongation at fracture was also found to be 2.74 %, 3.12 % and 5.50 % in CPHZ I, CPHZ II and CPHZ III respectively. Moreover, good antimicrobial effect was observed for CPHZ I-III against three different bacterial strains. Overall, percentage porosities and tensile strength of CPHZ I-III were in the range of cancellous bone. Hemolysis assay showed that there was no damage of erythrocytes in presence of CPHZ I. Good biodegradability of the nanocomposite was also observed by *in vitro* degradation study in physiological-like conditions. Most importantly, these nanocomposites benefit for the osteoblast-like cells growth, attachment and proliferation, had no negative effect on osteoblast-like MG-63 cells and showed good cytocompatibility. All the above results suggest that these nanocomposites have a great potential to be used as bone tissue engineering materials.

Notes and references

[a]Department of Polymer Science and Technology, University of Calcutta, 92 A.P.C. Road, Kolkata-700009, India.

[b]Microbiology Division, CSIR-Central Leather Research Institute, Adyar, Chennai-600020, Tamil Nadu, India.

ᶜDepartment of Chemical Engineering, University of Calcutta, 92 A.P.C. Road, Kolkata-700009, India.

*Corresponding author. Email- ppk923@yahoo.com.

Phone: +91-33-2352-5106.

1. L. L. Hench, *J. Am. Ceram. Soc.* 1998, **81**, 1705.

2. L. P. Madalina, M.P. Roxana, P. Stefania, Z. Livia, M. Ion, S. Gabriel and L. Witold, *Rev. Adv. Mater. Sci.*, 2004, **8**, 164.

3. S. Miao, W. Weng, K. Cheng, P. Du, G. Shen, G. Han and S. Zhang, *Surf. Coat. Tech.*, 2005, **198**, 223.

4. G. Mestres, C. Le Van and M. P. Ginebra, *Acta Biomater.*, 2012, **8**, 1169.

5. A. Ito and M. Otsuka, *Curr Appl phys*, 2005, **5**, 4026.

6. R. Z. Legeros, *US Patent* 2008, **7**, 419, 680.

7. C. Deepa, A. Nishara Begum and S. Aravindan, *Nanosist.: fiz. him. mat.*, 2013, **4**, 370.

8. C. Du, F. Z. Cui, W. Zhang, Q. L. Feng, X. D. Zhu and K. De Groot, *J Biomed Mater Res A* 2000, **50**, 518–27.

9. M. Kikuchi, S. Itoh, S. Ichinose, K. Shinomiya and J. Tanaka, *Biomaterials* 2001, **22**, 1705.

10. K. Ogawa, S. Hirano, T. Miyanishi, T. Yui and T. A. Watanabe, *Macromolecules*, 1984, **17**, 973.

11. K. Okuyama, K. Noguchi, Y. Hanafusa, K. Osawa and K. Ogawa, *Int. J. Biol. Macromol.*, 1999, **26**, 285.

12. A. Sionkowska, *Prog. Polym. Sci.*, 2011, 36, 1254.

13. R. A. A. Muzzarelli, M. Mattiolibelmonte, C. Tietz, R. Biagini, G. Ferioli, *Biomaterials* 1994, **15**,1075.

14. J. Y. Lee, S. H. Nam, S. Y. Im, Y. J. Park, Y. M. Lee, Y. J. Seol, C. P. Chung, S. J. Lee, *J Control Rel*, 2002, **78**,187.

15. N. Shanmugasundaram, P. Ravichandran, P. Reddy, N. N. Ramamurthy, S. Pal and K. P. Rao, *Biomaterials*, 2001, 22, 1943.

16. S. B. Bahrami, S. S. Kordestani, H. Mirzadeh and P. Mansoori, *Iran. Polym. J.*, 2003, **12**, 139.

17. L. V. Schueren, I. Steyaert, B. Schoenmaker and K. Clerck, *Carbohydr. Polym.*, 2012, **88**, 1221.

18. K. Desai and K. Kit *Polymer*, 2008, **49**, 4046.

19. K. S. V. K. Rao, P. R. Reddy, Y.Lee and C. Kim, *Carbohydrate Polym.*, 2012, **87**, 920.

20. S. D. Jazayeri, A. Ideris, Z. Zakaria, K. Shameli, H. Moeini, A. R. Omar, *J. Control Release*, 2012, **161**, 116.

21. N. Pramanik, P. Bhargava, S. Alam and P. Pramanik, *Polym. Compos.*, 2006, **27**, 633.

22. M. Boissiere, P. Z. Meadows, R. Brayner, C. Helary, J. Livage and T. Coradin, *J. Mater. Chem.* 2006, **16**, 1178.

23. X. Zhang, D. Yang and J. Nie, *Int. J. Biol. Macromol.*, 2008, **43**, 456.

24. M. Guiping, Y. Dongzhi, L. Qianzhu, W. Kemin, C. Binling, F. K. John and N. Jun, *Carbohydr. Polym.*, 2010, **79**, 620.

25. M. Freyman, I. V. Yannas and L. J. Gibson, *Prog. Mater. Sci.*, 2001, **46**, 273.

26. J L. Sang, J. L. Grace, J. W. Lee, A. Anthony and J. Y. James, *Biomaterials*, 2006, **27**, 3466.

27. K. Rezwan, Q. Z. Chen, J. J. Blaker and A. R. Boccaccini, *Biomaterials,* 2006, 27, 3413.

28. K. Sahithi, M. Swetha, M. Prabaharan, A. Moorthi, N. Saranya, K. Ramasamy, N. Srinivasan, N. C. Partridge and N. Selvamurugan, *J. Biomed. Nanotechnol.*, 2010, **6**, 333.

29. A. Bhowmick, R. Kumar, M. Das and P.P. Kundu, *Adv. Polym. Tech.*, 2013, **33**, 1391.

30. S. Banerjee and A. Saha, *New J. Chem.*, 2013, **37**, 4170.

31. A. Singh, R. Kumar, N. Malhotra and Suman, *Int. J. Sci. Emerg. Technol. Latest Trends*, 2012, **4**, 49.

32. W. W. Thein-Han and R. D. K. Misra, *Acta Biomater.*, 2009, **5**, 1182.

33. M. B. Ahmad, K. Shameli, M. Y. Tay, M. Z. Hussein, J. J. Lim, *Res. Chem. Intermed.*, 2014, **40**, 817.

34. E. Wintermantel, J. Mayer, J. Blum, K. L. Eckert, P. Lüscher, M. Mathey, *Biomaterials*, 1996, **17**, 83.

35. J. F. De Oliverira, P. F. De Aguiar, A. M. Rossi, G. A. Soares, *Artif. Organs.*, 2003, **27**, 406.

36. H. Liu, T. J. Webster, Nanotechnology for the Regeneration of Hard and Soft Tissues, Webster TJ (ed), World Scientific, 2007, 1-52.

37. S. Kundu, M. Mandal, S. K. Ghosh and T. Pal, *J. Colloid Interface Sci.*, 2004, **272**, 134.

38. N. Saranya, S. Saravanan, A. Moorthi, B. Ramyakrishna and N. Selvamurugan, *J. Biomed. Nanotechnol.* 2011, **7**, 238.

39. H. Liu, J. Mao, K. Yao, G. Yang, L. Cui and Y. Cao, *J. Biomater. Sci. Polym. Ed.*, 2004, **15**, 25.

40. R. Hodgkinson and J. D. Curry, *Proc. Inst. Mech. Eng. [H]* 2002, **204**, 115.

41. V. Deepak, P. S. Umamaheshwaran, K. Guhan, R. A. Nanthini, B. Krithiga, N. M. H. Jaithoon and S. Gurunathan, *Colloids and Surfaces B: Biointerfaces* **2011**, 86, 353.